

MANUFACTURING AND ECONOMIC CONSTRAINTS ON THE STRUCTURAL DESIGN OF A REDUCED- SIZED TECHNOLOGICAL DEMONSTRATOR

E. Carrera*, S. Chiesa*, S. Corpino*

***Department of Aeronautics and Space Engineering
Politecnico di Torino**

*Corso Einaudi, 40, 10129 Torino, Italy
+39-011-5646858*

erasmo.carrera@polito.it; sergio.chiesa@polito.it; sabrina.corpino@polito.it

Keywords: *technological demonstrator, structural design, manufacturing, affordability*

Abstract

In collaboration with the Italian Aerospace Research Centre (CIRA), our research group has carried out the conceptual design of a small technological demonstrator (called mini-FTB) oriented towards the execution of a Sub-orbital Re-entry Test mission (called mini-SRT).

Main target of the mini-SRT mission is to improve technological and scientific knowledge useful to reduce risks connected to the SRT mission settled by CIRA to be flown by a Flying Test Bed (FTB2) of considerable size and sophistication.

The present work deals with the problems encountered while developing the layout of the mini-FTB and in particular its structural frame. The architectural configuration of the demonstrator is constrained by the following specifications:

- *It must be similar to the FTB2 developed by CIRA;*
- *It must take into account the interface between the demonstrator and its carrier, that is a stratospheric balloon, and between the demonstrator and its booster;*
- *It must be easily and affordably built and assembled.*

The mini-FTB is constituted by the demonstrator and the booster attached at the rear part of the fuselage. The total length of the demonstrator is about 1.5 meters, while the weight is about 50 kg. The scale factor between the mini-FTB and the original FTB2 is 1:5.

The structural design of the mini-FTB is quite interesting. In fact, due to the requirement of affordability, it is driven by considerations like the employment of low-cost materials and construction technologies. On the other hand, the severe thermal and acceleration conditions must be taken into account. The choice of the materials to be employed as thermal shield is driven by the results obtained from the structural analysis performed on each part of the demonstrator. The structural analysis has been carried out through a FEA program to know the structural response of the mini-FTB.

Original manufacturing processes have been adopted in order to lower the cost. The entire manufacturing and assembly process will be described in detail in the paper.

The mini-SRT program is also characterized to be a short-term project. This fact has implied to avoid time-consuming calculations and unnecessary activities. The mini-FTB design has carried out till the subsystems level and their installation into the airframe. The integration activity has turned out to be quite critical. Due to the high g-level reached during the propulsion and the re-entry phases, the connection between the subsystems components and the structural elements must be investigated into details and it represents an important constraint for the design of the structure.

The paper will examine thoroughly the problems cited here.

1 Program objectives

The main program objective is to demonstrate the feasibility of a drawn to scale demonstrator, able to perform at least partially the third USV mission (scheduled by CIRA in PRORA-USV research program [1]), named SRT, characterized by the following objectives:

- To get technological and operational know-how for the crucial re-entry phase;
- To verify the operational procedures necessary for a system constituted by a stratospheric balloon and a propelled vehicle, the mini-FTB;
- To examine the mechanical interface between the mini-FTB and the balloon and to study their separation phase;
- To test the Guidance, Navigation and Control System (GNC);
- To verify the control laws of hypersonic flight;
- To define an accurate aerodynamic database in supersonic and hypersonic regimes;
- To measure significant environmental parameters;
- To guarantee an adequate safety level;
- To design and build a reusable test vehicle.

This demonstrator must be small (approximately 1.5 meter long), light (50 kilograms maximum mass) and affordable. It must be able to gain operative and technical confidence on re-entry aspects by collecting experimental data, to test in-flight hypersonic GN&C control techniques and to test advanced materials under severe conditions. Another useful objective is the identification of problems that the main mission will probably face, especially as far as concerns the balloon separation phase [2] [3] [4].

2 Structural Design

The driving factor of the Mini-FTB structural design, in compliance with the philosophy of the project, is to keep cost as low as possible to satisfy design requirements. Commercial off the shelf materials have been widely used, as well as state of the art technologies. The Mini-FTB has been designed

to be constituted by four main parts to be assembled:

- forward body
- wing/main body
- rear body/empennages
- power system

In the following figure (Fig. 1) the four parts are illustrated by means of a CAD model. The detailed description of the four parts is in the next paragraphs.

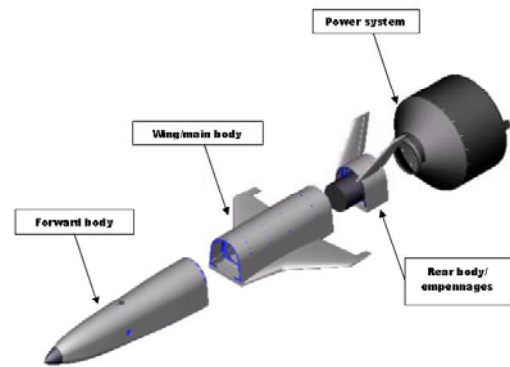


Fig. 1: Mini-FTB layout

In Figure 2 the Mini-FTB structure layout without power system and external skin is shown.

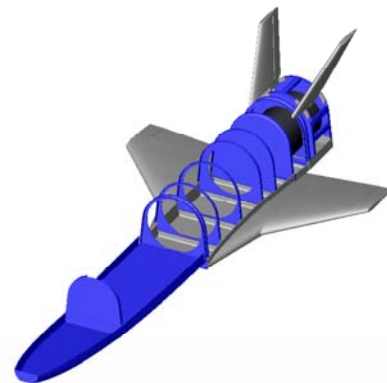


Fig. 2: Mini-FTB structure layout

2.1 Forward body

The forward body consists of the nose and of the forward part of the Mini-FTB. It is constituted by two floors, dedicated to house onboard systems and two frames (one dedicated to the attachment to the wing/main body and the other dedicated to the attachment to the group of thrusters). The selected material for the floors is stainless steel. The internal structure is bolted to

the external skin and it is separated from it by means of a felt sheet. The external skin is made of Incoloy® MA956. A thermal barrier coating is used as Thermal Protection System (TPS). See figure 3.

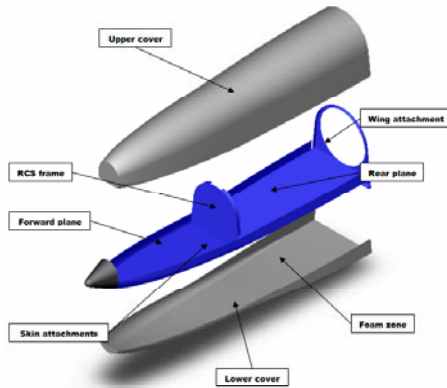


Fig. 3: forward body layout

2.2 Wing-main body

The structure of the wing/main body is similar to the one of the forward body. All parts not directly exposed to the external flux are made of stainless steel, whereas the external skin, wing and control surfaces are in super alloy Incoloy® MA956, coated with Thermal Barrier Coating (TBC).

All internal frames, besides accomplishing structural functions, are the attachment points for related components and connections between the forward and the rear body. Starting from the nose, the first frame is dedicated to the forward body attachment (nose attachment frame). The following three frames are used for the Reaction Control System (RCS) (tank frames). The electrical motors and the RCS thrusters are connected to the fourth and fifth frames (actuators frame and RCS frame), while the last one is dedicated to the attachment to the empennage/rear body part (empennages attachment frame). The holes are necessary to make room available and to allow pipes crossing. All frames are sheltered from hot components by means of felt sheets, while the void areas are filled with foam.

The wing spars help distribute loads and create attachment points for frames. The rear edge of the wing is machined in order to get the elevons hinge. The control surfaces are

activated by a torsion tube. The main and wing body part is illustrated in the figure below.

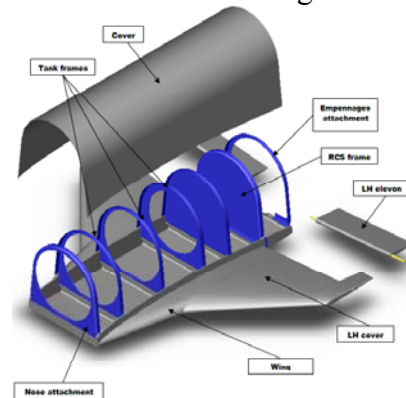


Fig. 4: main body layout

2.3 Rear fuselage/empennage and power system

Main tasks of the rear fuselage are not only the empennage installation but also the connection between the engine and the demonstrator, the loads distribution from the rear frame to the overall demonstrator structure and the parachute housing.

The parachute is deployed along the longitudinal axis, for availability of room and ease of use, thus implying cost reduction. The selected configuration also guarantees a stable configuration during re-entry when the parachute is opened. Figure 5 shows an exploded view of the empennage/rear body.

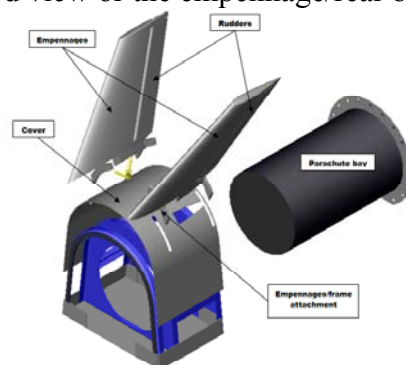


Fig. 5: rear body exploded layout

All wet surfaces are made of super alloy: the empennages, the control surfaces, the rear floor, the external covering and the last frame. The internal frames and the parachute container are made of stainless steel. All the external parts are coated by TBC. The first frame has the duty

of connect the rear body with the central body (wing attachment frame). The subsequent two frames are dedicated to connect the parachute container and the empennages: they are interconnected by means of two longitudinal reinforcements and are fixed to the external cover. The main task of the longitudinal reinforcements is to transfer the engine thrust to the demonstrator in order to avoid the collapse of the rear structure. The empennages are bolted to the forward frame by a dedicated attachment. In order to get the rudder hinge, the rear edge of each empennage is machined. The control surfaces are activated by a torsion tube similar to the one adopted for the elevons. In the next figure the adapter for engine attachment is detailed. The assembly is fixed by means of a “Marmor” belt, usually used in aerospace for stage separation of launch vectors (Fig. 6).

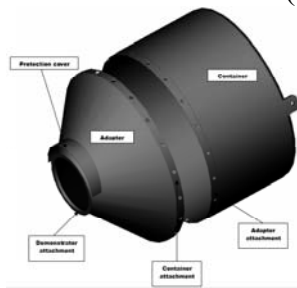


Fig. 6: adapter and container for engine

3 Manufacturing

3.1 Objectives

One of the main objectives of the project was the evaluation of the problem related to the final assembly of the demonstrator and the research of the appropriate methodologies in order to minimize the working time [6]. Outputs of the investigation have been:

- Manufacturing plan of the demonstrator structure and related “part list”;
- Assembly and disassembly process definition.

3.2 Frames

In the preliminary design, the frames (Fig. 7) are made by formed sheets of stainless steel

AISI 316 - 1 mm thick, with the exception of the last frame that is 2 mm thick. The analysis of the assembly details could lead to the consideration that some frames could be made in more economical way by C/N machined plates instead of by formed sheets.

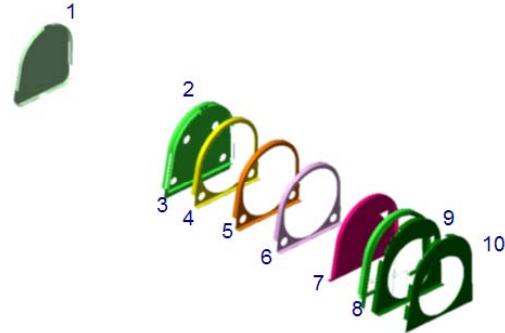


Fig. 7: Mini-FTB frames

The preliminary design shows that although similar in shape and dimensions, all the frames are geometrically different. If only one jig has to be used, the bending mould must have the possibility of increasing/decreasing the dimensions of matrix and bending stamp and of moving the reference points according to the shape of each frame. Moreover, a precise manufacturing plan has to be designed and adopted. The proposed manufacturing plan is described below.

The first step consists of unwrapping the frames, in other words “to open up” all flaps designed for assembly purpose. The frames 2-3-8 have the same shape and the flaps are turned into the same direction. The other frames (except for frame number 1) have the flaps on the base and the lateral flaps turned into the opposite direction. From this analysis it is possible to build a bending mould which first bends the frames number 2-3-8 and then the remaining frames number 4 to 10. Figure 8 shows the configuration of the mould, named A, which is suitable for frames number 2-3-8. As consequence of the reduced dimensions of the number 1 frame, notwithstanding the similarity with the other frames, it is necessary to build a dedicated mould. Here is a table showing the manufacturing process of the frames:

FRAMES	MANUFACTURING PLAN
No. 2-3-8	<ul style="list-style-type: none"> ▪ laser cutting of the external profile ▪ flap bending using A configuration mould ▪ laser cutting of holes and edges
No. 4-5-6-7-9-10	<ul style="list-style-type: none"> ▪ laser cutting of the external profile including internal holes ▪ flaps bending using the mould in B configuration ▪ nose, fuselage-wing flaps bending using "V" mould
No. 1	<ul style="list-style-type: none"> ▪ laser cutting of the external profile ▪ flap bending using a dedicated mould ▪ laser cutting for holes and edges

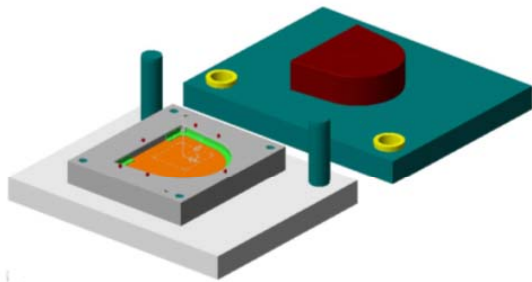


Fig. 8: Mould A for frames 2-3-8

3.3 Wing/main body

The machined part of the wing/main body consists of integral spars that, starting from the wing and continuing inside the fuselage, are also used as frame attachments.

The part, made by C/N machining, shows a complexity of fabrication due to the particular material used (Incoloy® MA956) that needs special tools. The starting plate is easily available, as COTS component, and its dimensions are: 700 x 700 x 50 mm. During the manufacturing drawing phase the mathematic of the part will be optimized for C/N machining. In particular all surfaces will be joined and negative angles of the spars and ribs will be eliminated. The machine tool suitable to accomplish the task is a 3 axes milling machine, but it is better to use a 5 axes milling machine. A proposed manufacturing plan is:

- *Rough material preparation.*
- *Clamping the holes.* The clamping main purpose is the vibration reduction of the part that has to be worked. The holes needed for clamping are made in two separated parts,

placed respectively forward and rearward of the fuselage.

- *Cutting, using circular saw, and removal of unused parts (Fig. 9).* These parts will be used for elevons manufacturing.

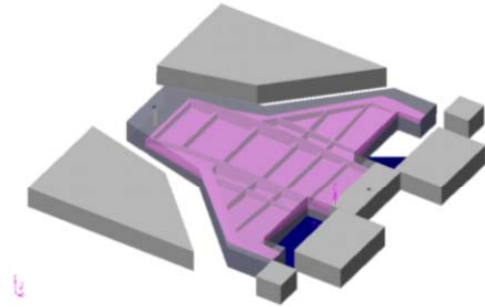


Fig. 9: first stages of manufacturing

- *Machining of the wing profiles.* The machining starts from external parts, because they present some difficulties and moreover a high precision is required. In this operation the use of a milling machine with 5 axes instead of 3 is mandatory. The plate is fixed to the milling machine using the fixing holes made in the previous operation. In figure 10 the CAM work is shown. After the upper surface machining is finished, the lower part has to be worked. A possible solution consists of preparing a formed positioning jig (but an expensive CAD design it is necessary) or a similar bed using epoxy resin (this alternative is considered more rapid ed economical.

- *Machining of lower wing/fuselage profiles.* The machining starts with a rough milling, followed by a final work using appropriate tooling.

- *Machining of elevon surfaces.* At this stage the shape of the part is completed with the exception of the areas in which the elevons are to be fitted. This operation requires some manual work as a consequence of the particular geometry.

- *Cutting of parts containing the fixing holes.* At the end of machining operations the fixing holes are not necessary anymore and the related parts can be eliminated. Some refinement works can be made, if needed.

- *Electro erosion technique* has been chosen for elevon attachment. For this operation an electro erosion machine is proposed in order to

achieve a high level of precision. A particular tool (copper electrode) is necessary for the process (Fig. 11).

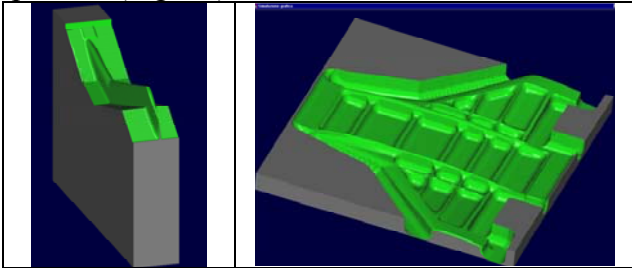


Fig. 10: CAD-CAM analysis

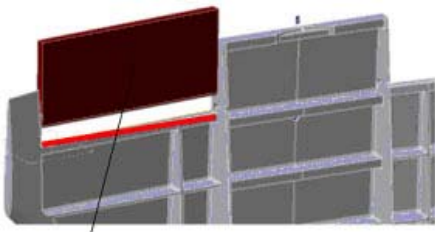


Fig. 11: elevons construction

The wing/central body is completed by means of the upper panel (1 mm thick) which constitutes the skin and it is made in stainless steel AISI 316. The final shape is imposed during the assembly phase by riveting/bolting the panel to the machined part (Fig. 12).

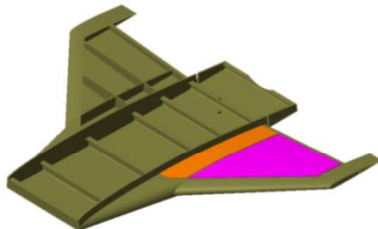


Fig. 12: final stage of central body manufacturing

3.4 Tail and nose floor

The tail floor is made by a box of austenitic stainless steel sheet AISI 316 - 2 mm thick. In order to cut the sheet 2 mm thick, the proposed methodology consists of the use of electro erosion or laser. Both technologies are “non conventional” mechanical operations used in aerospace field. Starting from the geometry of the unwrapped box, some problems may arise during the bending of flaps named Y in the figure 13, because after the bending they show an angle less than 90° . The problem can be

solved by the employment of a particular device and by the appropriate operations’ sequence.

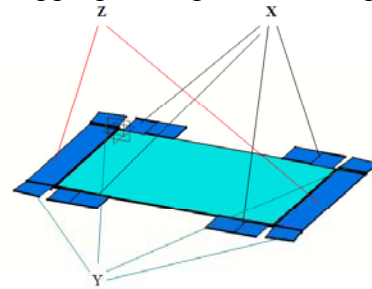


Fig. 13: tail unwrapped box floor

The flaps X have to be bent first, then the Y flaps. Eventually the flaps Z have to be bent. The floor of the Mini-FTB forward part is composed by two parts: they form the basis for the flight equipments installation. Both floors are made by austenitic stainless steel sheet AISI 316 - 1 mm thick. From CAD analysis, it arises that both parts, after the bending, show an angle less than 90° . It is possible to solve the problem by the use of a particular mould made by more than just one piece. The design and construction of such device is complicated and expensive. It is possible to employ prototyping methodologies.

3.5 Tail and fuselage cover

The tail and fuselage covering are described together because the manufacturing methodology is the same. Both parts are made by austenitic stainless steel sheet AISI 316 - 1mm thick.. The first operation consists of obtaining the shape of the part, then the sheet is cut by using electro erosion machine. The final form of the part is obtained by using a dedicated mould (Fig. 14).

3.6 Elevons

The Mini-SRT is equipped with two elevons. The material selected is the super alloy heat resistant Incoloy® MA956. Alternative material is the titanium alloy. Considering the elevon dimensions (length and thickness) the C/N machining method is not suitable. The proposal is the use of electro erosion technique that permits to obtain good finishing in short time.

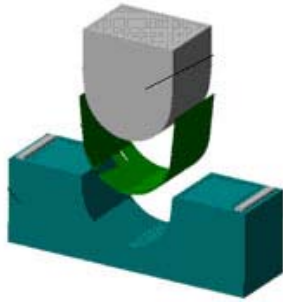


Fig. 14: manufacturing of the body cover

3.7 Machined details

In this paragraph some details necessary for the assembly of the demonstrator and not yet described are analysed. In order to connect the Mini-SRT wing/main body with the rear fuselage an L section beam is used. This beam, with appropriate bending, is attached to the last main frame of the fuselage. The beam is made by stainless steel - 1 mm thick. A dedicated mould is necessary in order to obtain the correct shape. In the rear fuselage, five longitudinal strengthening elements are foreseen, having the purpose of joining the two tail frames. The structural function of those longitudinal elements is the distribution of the thrust from the booster to the structure of the demonstrator. The strengthening elements are made by C profile of stainless steel sheet metal 1 mm thick. The cut is made by precise electro erosion technology. In order to achieve more resistance it is suggested to complete the work with a welding of the end area

3.8 Assembly sequence

In this paragraph, one of the possible assembly sequence of the Mini-FTB is proposed. The sequence starts from the rear fuselage, in particular from the open box previously described. At the end of the box frame 10 is attached. The frame shows a big central hole, necessary for the installation of the parachute system. A second frame is installed and, as the previous one, is considered as bulkhead frame because the empennages transfer their loads upon them. The next step is the introduction of the longitudinal

strengthening elements and the empennage assembly. The rudder is inserted in the fin by a pin. The assembly is completed by the insertion of a cardan joint. After the completion of the assembly of the second empennage, both empennages are attached to the frames. The assembly of the wing/main body starts from the machined part previously described. The assembly of elevons is made by using the technology employed for the rudders. Then the two frames (forward and rear) are installed. At this stage the subassembly appears as shown in figure 15. The next step is the installation of the engine mounting. The assembly is possible using the big hole in the frame. The attachment is made by a L-channel. It is possible to proceed to the installation of the remaining frames and of the gas tank that is fixed to the frames. For the front fuselage subassembly, the starting point is the RCS frame to which the two floors previously made are connected. Then the front fuselage is attached to the central and rear subassembly. Before the assembly of the lower skin is made, a foam is spread between the floor and the cover. At this stage the assembly is illustrated in figure 16.

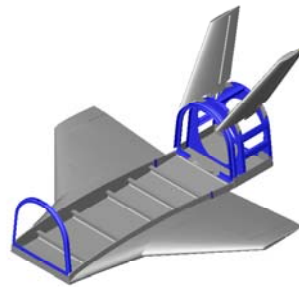


Fig. 15: initial assembly stage

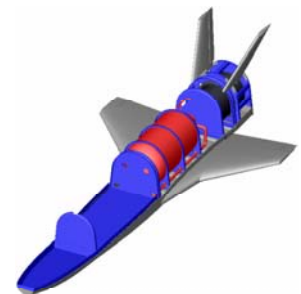


Fig. 16: intermediate assembly stage

The demonstrator can now be closed by using the covering sheets. The installation of the parachute and the frangible panel is the last operation. In parallel with the Mini-FTB assembly, the assembly of the engine is made. The STAR 17 is housed in the adapter and the Mini-FTB is now completed as shown in figure 17.

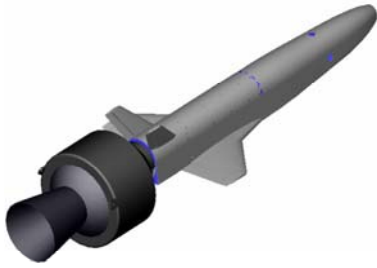


Fig. 17: final assembly stage

4 Materials and TPS

To build the airframe an iron-chromium alloy has been chosen. It is called Incoloy® MA956, and it is strengthened by additions of aluminium, titanium and yttrium oxide (Y_2O_3), to improve its thermo mechanical characteristics. It is produced by the mechanical alloying of metal powder process rather than by conventional melting. This super alloy has been set-up for aerospace applications and it is especially used for gas turbine combustion chambers. Despite its very good performances, its operational temperatures are not higher than 1300 °C. Due to the high temperatures of gas turbine combustion chambers, the thermal protection system for turbine blades is a well known topic. The so called Thermal Barrier Coating (TBC), widely used in turbine technologies when temperatures rise above certain levels, have now been employed for decades either to extend the turbine life cycle or to increase operating temperature of super alloy components. This technology can thus be utilized as thermal protection system of the demonstrator. In order to avoid the contact between the hot external superficial air flux and the demonstrator's body, the Thermal Barrier Coating is uniformly spread on the super alloy surface. A so called "bond coat" is usually placed between the top coat, the actual TBC, and the super alloy to enhance adherence. The most widely used material for TBC of turbine components is the partially stabilized zirconia (PSZ), made of ZrO_2 which is stabilised by the addition of Y_2O_3 , CeO_2 or MgO . This material is characterized by a small thermal conductivity (it is about 15% of that of the Incoloy® MA956,

which is $10,9 \text{ W m}^{-1} \text{ K}^{-1}$ at 25 °C) and at the same time by a high refractoriness. The PSZ also presents an acceptable fracture toughness value and its linear thermal expansion coefficient is comparable to that one of the Incoloy® MA956. This characteristic reduces the risk connected with the delamination of the ceramic layer deposited at the interface with the metallic substrate. The TBC is usually spreaded on the superalloy surface by a thermal spraying. The industrial widespread technique is the APS-air plasma spraying. Usually, the TBCs realized by an APS process have a standard thickness of about 200-300 μm . The surface roughness is estimated to be about 10 μm , the delamination strength at the interface between the TBC and the metallic coat is around 20-40 MPa and the Young's Modulus about 200 GPa. The mean thermal conductivity at 25 °C is around $0,8-1,1 \text{ W m}^{-1} \text{ K}^{-1}$, and it could be reduced by choosing appropriate commercial zirconia powders added with different percentage of Y_2O_3 . If the operational temperatures would raise up to very high values, the TBC made of PSZ could be inadequate for some components (nose, wing leading edge) which are stressed more than any other. Those elements can be made with special materials and then joined to the metallic structure. Between those materials, ceramic matrix composites (CMCs) appear to be adequate. The most used CMCs are non-oxide type, which can guarantee mechanical and thermal stability up to 1800 °C but for which a protective coat must be considered. Two major problems arise related to CMCs employment:

- the manufacturing of CMCs components of different shapes and geometry;
- the connection between the CMCs components and the main structure, in order to reduce heat exchange.

The modified relationship of Fay-Riddell has been compared with computational analyses and it is reliable for the estimation of thermal fluxes both on the nose and on the leading edge of the wing.

The mission requirement USV-SRT_1-USV_2-MSN-0040A "Atmospheric flight thermal requirements" has been satisfied by the

Mini-FTB/A configuration with a bending radius of 2 mm (i.e. drawn to 1:5 scale with FTB-2). The Mini-FTB configuration can not satisfy the previous requirement, but can achieve the desired density of thermal flux, i.e. 350 kW/m^2 . For most configurations the TPS made by PSZ spread by APS technique on the super alloy Incoloy® MA956 is suitable. Only the Mini-FTB/A configuration needs a ceramic nose, whereas the remaining body can be made of super alloy with a PSZ-based TPS (Fig. 18)

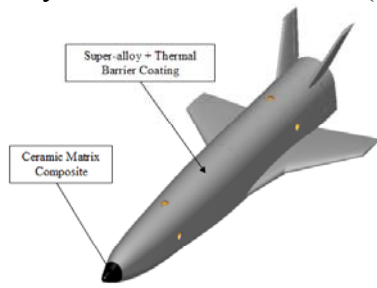


Fig. 18: TPS

5 Structural Analysis

Aim of this study has been the accomplishment of the demonstrator's structural analysis in order to verify the feasibility of the structural layout and weights breakdown. The selection of materials has also been verified.

The method used to perform the analysis has been the Finite Element Method (FEM), based on the demonstrator's CAD model. The NASTRAN® code has been used to carry out the analysis [7] [8].

The use either of two-dimensional or three-dimensional element depends upon which part of the vehicle has been considered: shells like the fuselage and the wing, having one dimension far smaller than the others, have been modelled by QUAD and TRIA while fuselage-wing attachments mainly by CHEXA and CPENTA.

5.1 Critical load cases

Figure 19 illustrates the demonstrator's trajectory. Thanks to the use of a simulation program, a first approximation of the structural loads applied during the mission has been made

and the most critical situations have been identified. As highlighted in the figure, three are the most critical cases from the structural point of view: the burn out, the maximum wing loading experienced during descent and the opening of the parachute. Extensive analyses have been carried out to verify the demonstrator's structural feasibility in those cases, when in-flight inertial loads, thrust and lift are applied. For each mission segment all loads applied have been considered in order to verify whether or not those loads can be carried by the vehicle and, if not, how the vehicle's structure itself can or must be modified.

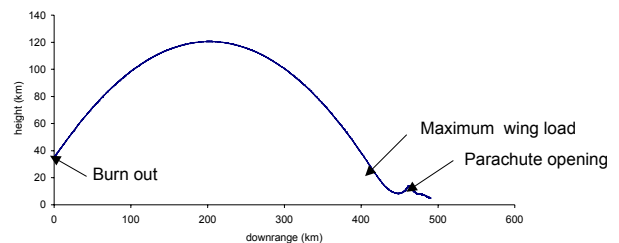


Fig. 19: Mini-FTB trajectory

5.2 The structural model

In figures 20 and 21 a comparison between the demonstrator's CAD and FEM models is shown. The wing shell, its spars and ribs, and the fuselage have been modelled by using bi-dimensional finite elements. As the fuselage is broken into two parts, the fore and aft fuselage, in order to connect these segments, elements characterized by infinite stiffness (RBE2) have been adopted, thus implying the same drift of the node which adjoins those elements. The FEM model of the wing-fuselage attachments has been built by using three-dimensional finite elements. In order to build a complete FEM model, all demonstrator's subsystems elements have been modelled. It has been already said about structural elements. Non structural components have been modelled by using scalar elements, CONM2, while their attachments to the demonstrator's skin and frames have been represented by RBE2 elements. Figure 22 shows how the various vehicle's subsystems components have been modelled in the FEM analysis; in particular, the element highlighted

in the figure constitutes the connection between fore and aft fuselage, modelled by RBE2 elements.

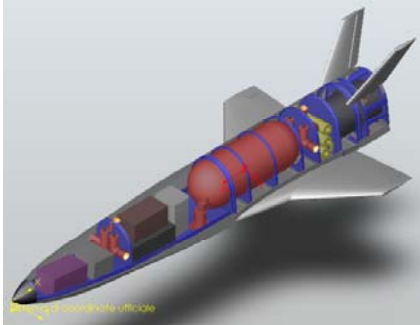


Fig. 20: Mini-FTB CAD model

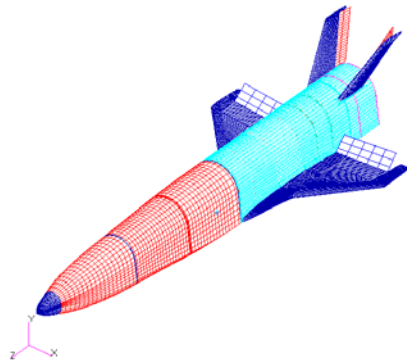


Fig. 21: Mini-FTB FEM model

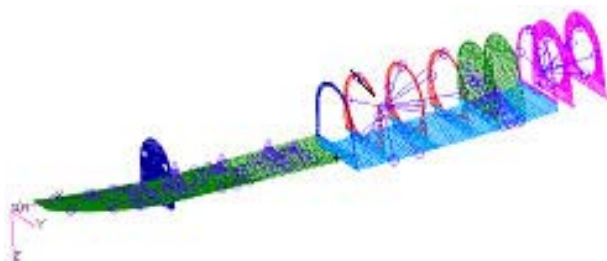


Fig. 22: FEM model of subsystem components

Listed below are the weights breakdown obtained by the CAD and FEM models and few more numerical data about the latter.

- Subsystems weight: 26.234 Kg;
- structural weight: 25.766 Kg;
- demonstrator weight: 53 Kg;
- number of elements: 32921;
- number of nodes: 29331;
- number of MPC: 111.

5.3 Stress analysis

After a first approximate analysis carried out by taking into account all possible loads, i.e. inertial, thrust and lift, as acting separately on

the vehicle, a different approach is considered. The three most critical cases, i.e. burn out, maximum wing load at descent and parachute opening, are studied and the relative structural analysis is accomplished.

5.3.1 In-flight inertial loads

The inertial in-flight loads are represented by the relative load factors. The maximum values of these loads, expressed in terms of acceleration in body axis reference frame, are:

- $N_x = 16360 \text{ mm/s}^2$;
- $N_z = -650 \text{ mm/s}^2$;
- $A_y = 1.33 \text{ rad/s}^2$.

The three accelerations listed above, have been first considered as if they were acting separately on the demonstrator, and then combined together.

5.3.2 Thrust

The thrust vector is applied along the vehicle's x-axis in the aft fuselage and it is considered as pressure uniformly distributed along the demonstrator's rear surface. The values of thrust, area and pressure are here listed:

- thrust, $T = 10834 \text{ N}$;
- area, $A = 19892 \text{ mm}^2$;
- pressure, $P = 0.546 \text{ Mpa}$.

The aim of the analysis is to verify whether or not the bundle of frames placed in the aft fuselage can carry the loads caused by thrust. As the results of the analysis show, the value of the stress tensor exceeds the limit of material only in one of the frames, the third one from the back, located in the aft fuselage. In order to overcome the problem, thicker two-dimensional finite elements, shell, can be adopted only for the above mentioned frame.

5.3.3 Lift

The lift is considered as pressure uniformly distributed along the demonstrator's wing upper surface. The values of lift, planform area and pressure for each half wing are here listed:

- lift, $L = 2000 \text{ N}$;
- planform area, $A = 187154 \text{ mm}^2$;
- pressure, $P = 0.0107 \text{ Mpa}$.

As the results show, there is a peak of the stress tensor where the wing attaches the

fuselage, but its value is so low as to warrant no attention from the structural point of view. Also the translational displacements of the wing and central part of the demonstrator's body have been evaluated. Their value is so low that reducing the number of frames inside the fuselage would not compromise the structure's behavior. The result of the structural analysis carried out so far shows that the values of the stress tensor caused by the lift force alone are not important.

5.3.4 Burn out

The so called burn out phase corresponds to the mission segment which starts when the Mini-FTB is dropped from the balloon and the rocket engine is fired and ends when the booster is relinquished. During this phase the most significant force applied to the demonstrator is the thrust vector together with the inertial loads caused by the high acceleration's values along the vehicle's axes. As the aerodynamic forces, lift and drag, are negligible if compared to thrust, they are ignored in the structural analysis that follows.

Listed below are numerical data of interest:

- n_x body: 16.36 mm/s²
- n_z body: -0.65 mm/s²
- Thrust: 10834 N
- Lift: 48 N
- Drag: 25 N
- Weight: 66.2 kg
- Angle of attack: 3.6°
- $\gamma = 38.4^\circ$

The result of the analysis is that the value of the stress tensor exceeds the limit of material only along the bundle of frames located aft fuselage. Moreover, the value of the translational displacements in the internal structural layout demonstrates the actual possibility to hold the various subsystems components inside the demonstrator's body.

5.3.5 Max wing loading during descent

During descent the only forces acting on the demonstrator's body are the aerodynamic forces, lift and drag, the latter being lower. As the wing is designed to carry the structural loading of shear, it has to be shown that the wing can carry the lift force.

Listed below are numerical data of interest:

- n_x body: -5.95
- n_z body: 9.57
- Lift: 4676 N
- Drag: 3153 N
- Weight: 47.4 kg
- Thrust: 0 N
- Angle of attack: 3°
- $\gamma = -23.7^\circ$
- Angular acceleration (pitch): 1.33 m/s²

If compared to the burn out case, the load factors are lower and the angular acceleration of pitch is now considered. As the value of the stress tensor is not so high, we expect to have acceptably small translational displacement.

5.3.6 Parachute opening

Opening the parachute implies the generation of a drag force of about 75000 N. As seen for the thrust, the above mentioned drag force is modelled as structural loadings of tension uniformly distributed along the rear vehicle's surface section. Being the area, on which the drag force is applied, 19892 mm², the tensions' value is 3.77 MPa. The highest values of the stress tensor are sensed by the third rear internal frame. In order to adequately withstand the structural loading of tension generated when the parachute is opened, the parachute attachments should be appropriately designed. A different solution could be the provision of an external structure to be placed aft fuselage with the purpose of collecting the forces generated by the parachute. The highest values of the translational displacements are sensed where the parachute is attached to the fuselage, and located along the aft fuselage, the internal bundle of frames, the fore and central horizontal plane and the whole demonstrator's body.

5.4 Structural analysis results

The structural analyses involving the lift force have shown that the demonstrator is subjected to so low stress tensors that the thickness of the whole structure or at least of the wing and central body can be smaller, thus implying a reduction of the structural weight

and an increase of the room available inside the body. Taking into account the limit of material of 655 MPa, notwithstanding the structural thickness reduction from 3 to 1.5 mm the values of the stress tensor are still reasonable.

To conclude, it can be said that the Mini-FTB, resulting from the preliminary design and first approximate weight estimation, appears to be able to withstand the loads applied during the various mission segments. Only few structural changes are required to reduce local high stress tensor values. The bundle of frames located in the aft fuselage needs to be modified. Not taking into account the critical case characterised by opening the parachute, the problems arisen during the structural analyses can be overcome simply by making the thickness of the third rear frame double. Please note that the mentioned third frame is the one where the highest values of the stress tensor are sensed.

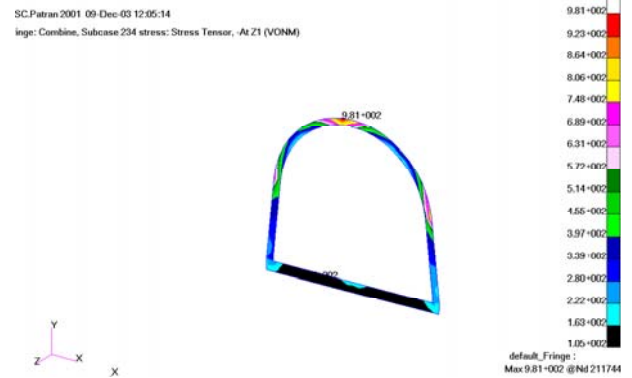


Fig. 23: stress tensor values on the third rear frame doubled

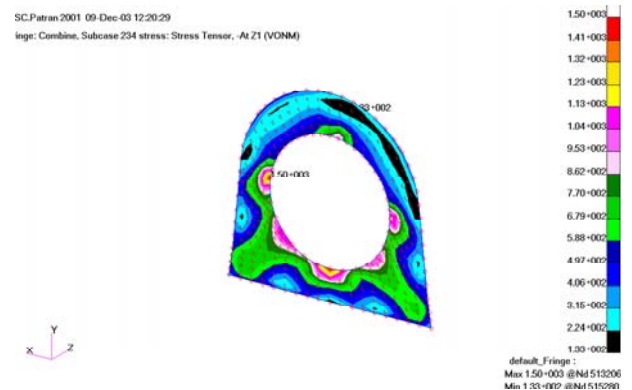


Fig. 24 stress tensor values on the most rear frame with the third rear frame doubled

The highest values of the stress tensor are lower (about 35% less) than the ones previously obtained and are now sensed where thrust is

applied, as illustrated in figure 23 and 24. Despite the decrease of the stress tensor's peak, the stress tensor values are still higher than the limit of material. To overcome the problem, the thickness of the aft frame, on which thrust is applied, has been doubled. A second structural analysis has been accomplished after making the above mentioned structural changes. See figures 25 and 26. The stress tensor values exceed the limit of material only where the central and the rear part of the demonstrator's body are attached, as showed in figure 27.



Fig. 25: stress tensor values on the most rear frame doubled

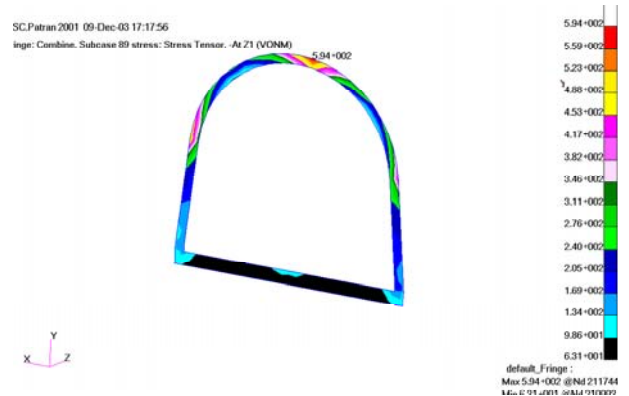


Fig. 26: stress tensor values on the third rear frame with the most rear frame doubled

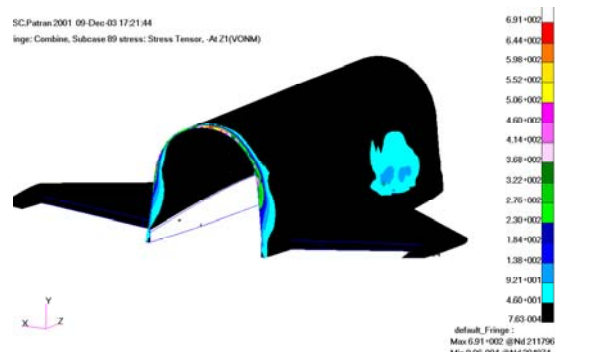


Fig. 27: maximum stress tensor values

To conclude it can be said that, by making the thickness of both the third and rear frames double, the stress tensor values are now about 50% less than the ones obtained before.

6 Cost estimation

In this paragraph a first approximate cost estimation of the demonstrator is presented. Unfortunately, it has not been possible to find an official quotation of all the equipments, then, for some of them, a rough estimation has been done.

Manufacturing cost	
Booster	TBD
RCS	450 k€
General system prime cost	100 k€
Material and structure	50 k€
Parachute	20 k€
TPS and TCS	5 k€
TOTAL	625 k€ + booster

The total cost of the demonstrator is driven by the cost of the RCS system and by the cost of the Power System (Fig. 28).

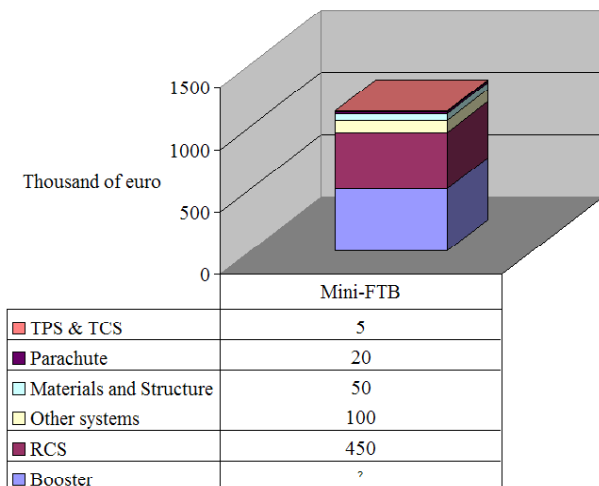


Fig. 28: demonstrator cost analysis

7 Conclusions

The study has demonstrated the feasibility of the Mini-FTB, as conceived to perform the Mini-SRT mission [5].

Acknowledgments

The authors are very grateful to Dr. Ing. Nicole Viola for her precious contribution.

References

- [1] Russo G.. Next generations space transportation systems. *Aerotecnica - Missili e Spazio*, Vol. 81, No.2, 2002.
- [2] Chiesa S., Corpino S., Viola N.. Feasibility study of a technological demonstrator of reduced size for suborbital flight. *Proceedings of 24th International Congress of the Aeronautical Sciences*, Yokohama, Japan, August-September 2004.
- [3] Chiesa S., Corpino S., Pasquino M., Viola N., Fiorio G., Milanese M., Masoero M., Silvi C.. Studio di Fattibilità per un Dimostratore Tecnologico Estremamente Economico di Velivoli Ipersonici. *Proceedings of the XVI National Congress AIDAA*, Palermo, Italy, September 2001.
- [4] Remiti F.. *Studio di fattibilità di un dimostratore tecnologico sub-orbitale di dimensioni ridotte*. Final project in Aerospace Engineering, Politecnico di Torino, July 2003.
- [5] Politecnico di Torino, Università di Napoli Federico II, Università di Roma La Sapienza. *Mini-SRT feasibility study-Technical final report*. April 2004.
- [6] Gallea F.. *Possibili studi di fabbricazione per un dimostratore ipersonico*. Final project in Aerospace Engineering, Politecnico di Torino, July 2003.
- [7] Triffiletti S.. “*Analisi strutturale agli elementi finiti di un mini dimostratore ipersonico*”, Final project in Aerospace Engineering, Politecnico di Torino, February 2004.
- [8] Chiesa S., Di Sciuva M., Testore L.. Launch Vehicles Conceptual Design and Structural Analysis: an Integrated Approach via FEM, *Aircraft Design*. No. 2, Elsevier Science, 1999.